IOP PUBLISHING JOURNAL OF PHYSICS D: APPLIED PHYSICS

J. Phys. D: Appl. Phys. **42** (2009) 135302 (7pp) doi:10.1088/0022-3727/42/13/135302

A vector model for analysing the surface photovoltage amplitude and phase spectra applied to complicated nanostructures

Ts Ivanov[1], **V Donchev, K Germanova and K Kirilov**

Faculty of Physics, Sofia University, 5, blvd. J. Bourchier, Sofia-1164, Bulgaria

E-mail: tsvetanivanov@lycos.com

Received 30 March 2009, in final form 12 May 2009
Published 11 June 2009
Online at stacks.iop.org/JPhysD/42/135302

Abstract

An approach is presented for comprehensive and reliable analysis of the surface photovoltage (SPV) amplitude and phase spectral behaviour in various semiconductor materials and structures. In this approach the SPV signal is represented as a radial vector with magnitude equal to the SPV amplitude and angle with respect to the x-axis equal to the SPV phase. This model is especially helpful in complicated nanostructures, where more than one SPV formation processes arises during the spectrum run. The value of the proposed model has been demonstrated by the successful explanation of seemingly contradictory SPV amplitude and phase spectra of AlAs/GaAs superlattices with embedded GaAs quantum wells, grown on different GaAs substrates. This has provided useful information about the investigated nanostructures. The need for simultaneous examination of both SPV amplitude and SPV phase spectra in order to obtain a correct understanding of the experimental data is emphasized.

(Some figures in this article are in colour only in the electronic version)

1. Introduction

Surface photovoltage (SPV) spectroscopy is a powerful non-destructive and contactless characterization technique, which has been successfully applied for characterization of different semiconductor bulk materials and nanostructures [1–6]. Due to its high sensitivity this technique can give important information about the electronic structure and optical properties of nanostructures even at room temperature [1, 7, 8]. The basic principles and applications of the SPV spectroscopy were discussed in review papers [1, 9]. SPV measurements are performed mainly by means of Kelvin probe or metal–insulator–semiconductor (MIS) structure operation modes [1]. Due to some advantages [1], the MIS mode has gained popularity and has been widely used in recent years [2–4]. However, there are still open questions in the analysis of the results obtained by the MIS technique. Usually, only the SPV amplitude spectrum is considered in the literature [10–15] and little attention is paid to the information that can be retrieved from the SPV phase spectrum. The SPV phase spectra have been discussed mainly in terms of relative changes of the phase at certain critical wavelengths without defining the zero phase value [16, 17]. However, in order to obtain a thorough understanding of the complex SPV generation processes in the sample, the amplitude and phase SPV spectra should be discussed together. In our previous paper [8], we have addressed two interesting questions, concerning the application of the SPV phase spectral measurements for characterization of bulk semiconductors and nanostructures. First, it has been shown that the sign of the bandgap-related knee in the spectrum of the SPV phase modulus is positive (negative) for downward (upward) surface band bending. Thus the analysis of this spectrum could be used as a handy tool for determining the semiconductor type (n or p). Second, it was found that for the case of non-linear recombination, the SPV phase spectrum can reflect the features of the absorption coefficient spectrum, which were known only for the SPV amplitude spectrum.

In this work we further explore and use the abilities offered by the SPV phase spectroscopy for characterization of complicated structures, in the light of the simultaneous analysis of the SPV amplitude and phase spectra. In order to achieve an easier and reliable analysis of the SPV amplitude

[1] Author to whom any correspondence should be addressed.

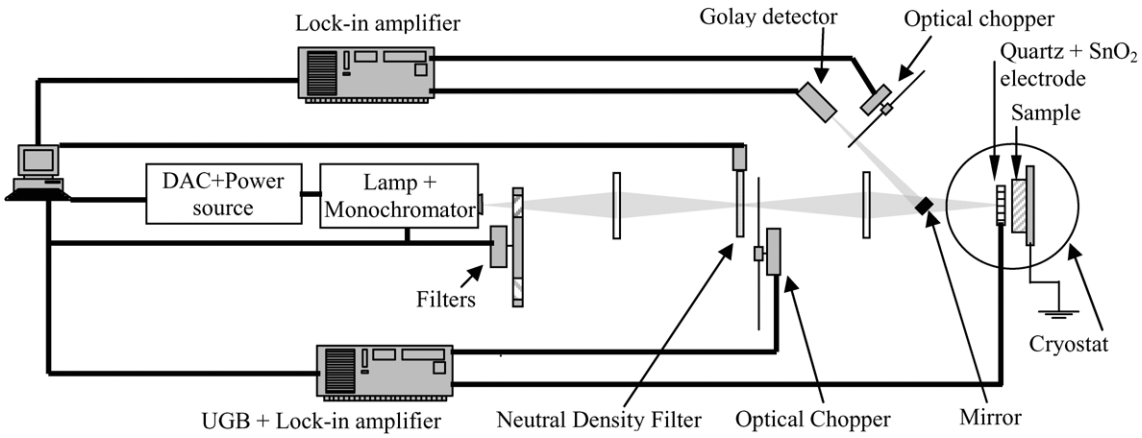

Figure 1. Experimental set-up for the SPV measurements.

and phase spectral behaviour we have developed a qualitative vector model, in which the SPV signal is represented by a radial vector, containing all the information given by the SPV amplitude and phase spectra. In order to demonstrate the applicability of the model we have measured the SPV amplitude and phase spectra of short-period AlAs/GaAs superlattices (SLs) with GaAs embedded quantum wells (QWs). These complicated nanostructures are interesting because they show a number of new physical properties, due to the interaction between the SL and the embedded QWs, as discussed in our previous studies of such systems, including photoluminescence and electronic structure calculation results [18–20]. They also have many advantages in comparison with single GaAs QWs with homogeneous AlGaAs alloy barriers [20], which makes them suitable for advanced devices fabrication such as QW lasers [21]. The application of the vector model to the present SPV amplitude and phase spectra has allowed us to understand and explain their complicated and seemingly contradictory behaviour. This has provided useful information about the investigated structures and at the same time presents an attestation of the applicability of the proposed model.

2. Experimental

2.1. Samples

The samples are grown by molecular beam epitaxy (MBE) at 600 °C on two types of (1 0 0) GaAs substrates: semi-insulating (SI) and Si doped ($1 \times 10^{18}\,\mathrm{cm}^{-3}$). They represent one GaAs QW of 5 nm (18 monolayers (ML), 1 ML = 0.283 nm) embedded between 20 (on top) and 26 (on bottom) periods of $(AlAs)_4/(GaAs)_8$ SL (4 and 8 are the number of MLs of AlAs and GaAs, respectively). There is a 50 nm cap layer of $Al_xGa_{1-x}As$ ($x = 0.33$, which is the mean Al content in the SL). No buffer layer is grown between the substrate and the first SL.

2.2. Experimental set-up

The SPV measurements are performed in the MIS operation mode [1]. The set-up is schematically shown in figure 1. The sample is mounted in a continuous flow optical cryostat. The semi-transparent electrode (probe) is a SnO_2 film deposited on quartz glass which presses the sample against a grounded copper platform.

The sample surface is illuminated by means of a 100 W halogen tungsten lamp along with a SPEX grating monochromator ($f = 0.22$ m), a filter to cut off the high-order diffraction and a PTI OC4000 optical chopper (94 Hz). The probe signal with respect to the ground is fed to a high-impedance unity gain buffer (UGB) and then measured by an EG&G 5207 lock-in amplifier. In order to achieve constant photon flux density ($\Phi \approx 1 \times 10^{13}\,\mathrm{cm}^{-2}\,\mathrm{s}^{-1} \pm 0.5\%$), part of the light incident on the sample is reflected with a small mirror towards a Golay detector (Oriel IR50), which has a flat response throughout the whole range of wavelengths used in the experiment. The reflected light is modulated with a second optical chopper (11 Hz) and the signal from the detector is fed to a second lock-in amplifier (Brookdeal 9530). This feedback is used to adjust the position of a neutral density filter with graded optical density, thus achieving a quasi-real-time control of the photon flux for each wavelength.

The SPV amplitude and phase measurement is performed as follows. The signal X, which is in phase with the reference signal from the first optical chopper, and the signal Y, shifted in phase by 90°, are measured and the obtained values are used to calculate the SPV amplitude A and phase φ by the following formulae: $A = (X^2 + Y^2)^{1/2}$ and $\varphi = \mathrm{arctg}(Y/X)$ (figure 2). Taking into account the signs of X and Y and the periodicity of the arctg function we obtain φ between −180° and +180°. The reference signal from the optical chopper defines the zero value of the SPV phase. For that purpose we have taken all measures to eliminate undesired phase shifts, following the procedures described in [8], which also have shown that the voltage transfer factor of the set-up is close to unity. All measurements are performed at room temperature with normal incident light, scanning from high towards low wavelengths.

3. Vector model for the SPV signal

As explained above the SPV signal is represented by its amplitude and phase and both their spectral dependences are

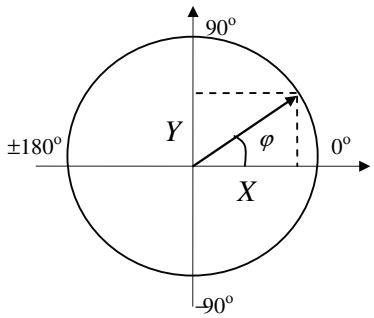

Figure 2. Representation of the SPV signal with a radial vector.

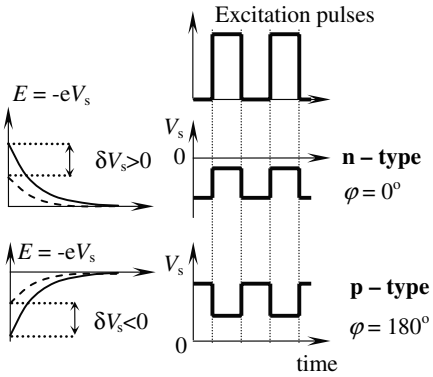

Figure 3. Left: surface band bending in dark (solid lines) and under illumination (dashed lines) of the conduction band edge in n-type (up) and p-type (down) semiconductors under depletion; Right: surface potential as a function of time in the case of n-type and p-type semiconductor compared with the light excitation pulses in the ideal case where no phase retardation exists.

recorded and give valuable information about the sample under study. This enables presentation of the SPV signal as a radial vector with the same magnitude as the SPV amplitude and angle with respect to the x-axis equal to the SPV phase (see figure 2). The SPV amplitude change leads to a change in this vector's magnitude, while the SPV phase change is represented by vector rotation.

The angle of the SPV vector, corresponding to a single SPV generation process, is related to the direction of the energy band bending at the position where it arises. For example, for a bulk semiconductor in dark with upward (downward) surface band bending with respect to the bulk, the surface potential V_s is negative (positive). The illumination decreases the surface potential in absolute value from $|V_s|$ to $|V_s^*|$ due to the redistribution of the photogenerated carriers by the built-in electric field. Hence, as discussed in [8] and represented in the left panel of figure 3, the change $\delta V_s = V_s^* - V_s$, which by definition is the SPV, is positive (negative). In the ideal case of very fast carrier generation, redistribution and recombination processes, which do not introduce any phase retardation of the SPV signal, the SPV phase, measured with respect to the light excitation, would be zero for upward band bending ($\delta V_s > 0$) and 180° for downward band bending ($\delta V_s < 0$), as illustrated on the right panel of figure 3. In the real case, due to the retardation of the signal with respect to the light excitation, the SPV phase, and consequently the angle of the SPV vector, is in the IV (II) quadrant for upward (downward) band bending.

In the case when only one SPV generation process is present, the increase in the carrier generation rate $\alpha\Phi$ (α is the optical absorption coefficient) will increase the SPV amplitude. The SPV phase will change if the system is in a non-linear recombination regime. Indeed, as explained in [8], increasing $\alpha\Phi$ leads to an increase in the excess carrier concentration $\Delta n(t)$ at a given moment t and consequently to a decrease in the momentary excess carrier lifetime $\tau(t) \sim 1/\Delta n(t)$ [22]. This will reduce the phase retardation of the SPV signal with respect to the light modulation and therefore will change its phase in the counterclockwise direction [8]. Consequently, in the case of the non-linear recombination regime, increasing the generation rate will not only increase the magnitude of the SPV vector, but will also rotate it counterclockwise. Eventually, for very high $\alpha\Phi$ the SPV process will reach saturation, and will become insensitive to changes in the generation rate.

This vector model is especially useful when more than one SPV formation process occurs in the spectrum run. A typical example is found in multilayered samples, where the absorption of the substrate and of the different layers usually results in SPV processes with different amplitudes and phases. Such a situation can be modelled by considering the addition of a second SPV generation process (with amplitude A_2 and phase φ_2) to an already existing one (with amplitude A_1 and phase φ_1).

Let us first consider a system which is and remains in linear recombination regime after the addition of the second process. If the phase difference $|\varphi_2 - \varphi_1|$ between the two SPV processes is less than 90° (acute angle or more precisely $|\varphi_2 - \varphi_1| < \arccos(-A_2/2A_1)$, which can be derived geometrically with the help of the cosine theorem), the addition of the second vector will result in a vector with larger magnitude, while if the angle is obtuse, the resulting magnitude will be smaller. In both cases the resulting vector will be rotated towards the second vector. Thus, both SPV amplitude and phase can change in both directions and one of the four possible combinations will take place, depending on the concrete amplitudes and phases of the two processes.

If one of the SPV generation processes involves non-linear recombination, the overall SPV phase spectral behaviour is influenced by both: the appearance of a second process (which can change the phase in both directions) and the non-linearity of the process (which changes the phase only in the counterclockwise direction with increasing $\alpha\Phi$, as discussed above).

We emphasize that the measurement gives the SPV signal, corresponding to the resulting overall vector (the vector sum of the vectors representing all the active processes) and deriving information about the individual processes requires further efforts. A quantitative analysis of the SPV vector addition requires assuming that the two processes are independent, which is a prerequisite for the validity of the superposition principle. As in the general case this is not strictly accomplished, we focus only on the qualitative analysis, so the proposed vector model is qualitative. Nevertheless, there are many cases in practice, where the dependence between the different processes is very weak and can be neglected. For example, the absorption of a thin QW leads to reduced

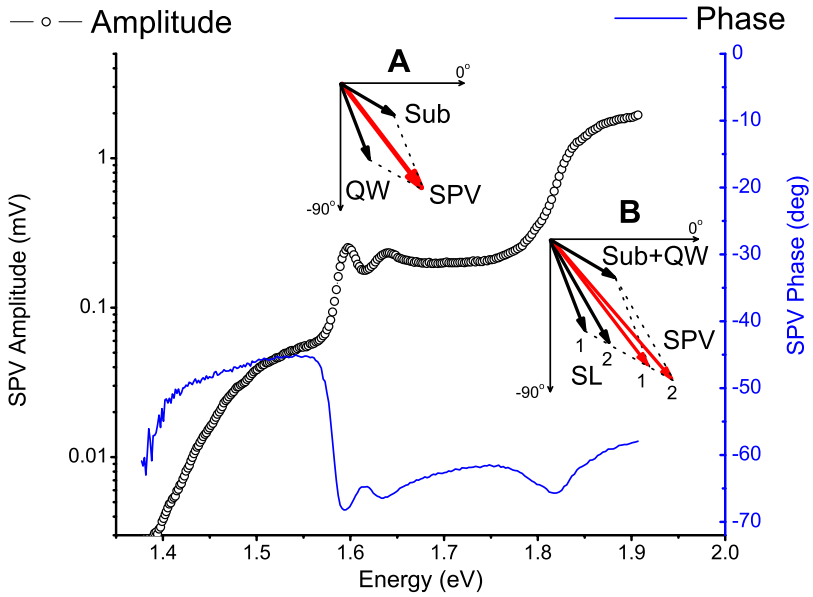

Figure 4. SPV amplitude (open circles) and phase (solid line) spectra of a sample grown on n-type substrate. Insets A and B—vector diagrams showing the interaction of different SPV processes for two different spectral regions. The overall SPV vector is shown in red. Sub, QW and SL denote the substrate, QW and SL vectors. (Colour online.)

photon flux density reaching the substrate and this way alters the substrate related SPV process. However, because of the huge difference between the QW and substrate volumes, this influence is small and could be neglected, especially in the case of non-linear recombination and saturation of the processes in the substrate. So, in similar cases quantitative calculations with the vector model will be possible and justified.

4. Results and discussions

The samples used in this study are identical structures (containing one GaAs QW embedded in AlAs/GaAs SL), which are grown on two different types of substrates and therefore differences in their SPV spectral behaviour are possible.

4.1. Samples grown on n-GaAs substrates

First we will discuss the samples grown on Si doped (1×10^{18} cm^{-3}) (0 0 1) GaAs substrate. Because the substrate is highly n-type doped and the rest of the structure is nominally undoped, the energy bands at the surface are bent upwards with respect to the bulk and a space charge region (SCR) develops. Thus, the SL, the QW and the AlGaAs cap layer are situated in a region with a built-in electric field oriented towards the surface, which contributes to the separation of the photocarriers and thus to the SPV signal formation. Figure 4 displays the typical SPV amplitude and phase spectra of these structures. The amplitude spectrum has been studied in our previous work [23], where all the spectral features have been identified based on comparison with PL investigations and envelope function approximation calculations.

The step in the range 1.400–1.550 eV in the amplitude spectrum (figure 4) originates from transitions in the GaAs substrate ($E_g = 1.424$ eV). In agreement with [8] and the discussion given in section 3, its n-type doping leads to an SPV vector in the IV quadrant (φ is around $-50°$). With an increase in the light energy the SPV amplitude increases due to the increased absorption. Simultaneously the SPV phase is almost constant in accordance with the linear dependence of the SPV signal on the photon flux density in this range (see figure 6(a)). Around 1.550 eV, both the SPV amplitude and the phase reach a nearly constant value, which is in accordance with the calculations and experimental results of other authors [24, 25]. The relatively low substrate contribution to the SPV is due to the high Si doping, which effectively screens the electric field and leads to a very narrow SCR situated mainly in the SL structure.

Above 1.550 eV the QW starts to absorb and its contribution to the SPV signal can be represented by a second vector again in the IV quadrant [8], due to the above depicted energy band bending in the nanostructure. As the overall SPV vector in this range experiences a clockwise rotation (φ decreases, see the solid line in figure 4), from the vector model it follows that the QW vector is closer to $-90°$ than the vector of the substrate (see inset A, figure 4). This means that the SPV process from the QW is slower as compared with the SPV process in the substrate. The amplitude spectrum in this range reveals two peaks ascribed to the E1-HH1 (1.597 eV) and E1-LH1 (1.639 eV) free exciton transitions in the QW similar to [23]. Accordingly, the SPV phase also exhibits two dips at very close energies (E1-HH1 at 1.593 eV and E1-LH1 at 1.635 eV), corresponding to clockwise rotation. The small difference in the energy position (4 meV) of these features between the amplitude and the phase spectrum can be explained by a slight counterclockwise rotation of the QW vector in addition to its magnitude change. Following the discussion in section 3, this rotation is in accordance with the slightly non-linear dependence of the QW related SPV amplitude on the photon flux density shown in figure 6(a).

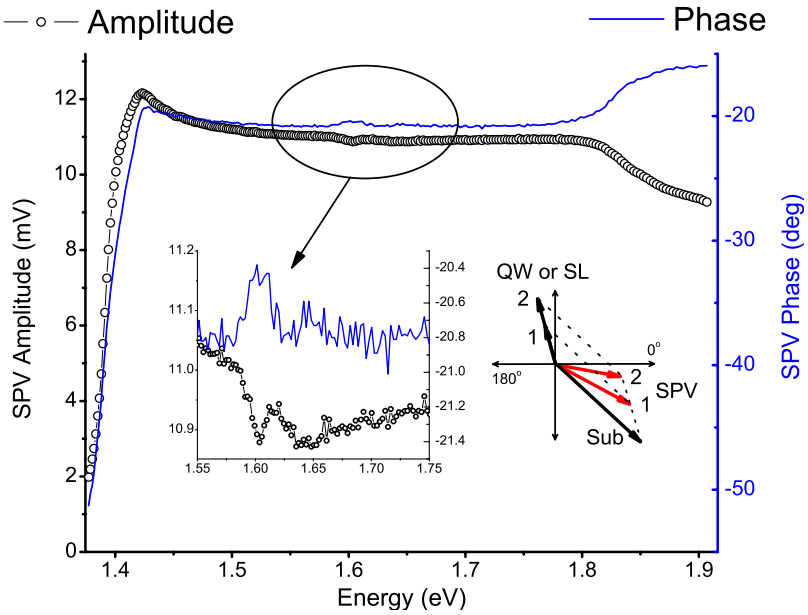

Figure 5. SPV amplitude (open circles) and phase (solid line) spectra of a sample grown on SI GaAs substrate. Insets: magnified amplitude and phase spectra in the QW energy range; vector diagram showing the dependence of the overall SPV vector (shown in red) on the growth of a vector in II quadrant (QW or SL absorption). (Colour online.)

After the peaks, the SPV amplitude has a constant value, which reveals the 2D density of states in the QW. Accordingly the SPV phase also remains nearly constant in this range.

Above 1.750 eV a step in the SPV amplitude spectrum is observed with an inflection point at 1.822 eV. This step is associated with transitions between the electron and the hole mini-bands of the SL [23]. The phase of the overall SPV signal is again in the IV quadrant in accordance with the direction of the energy band bending [8]. It first shows clockwise vector rotation (φ decreases) as in the QW region, but after 1.820 eV anticlockwise rotation starts (φ increases), while the SPV amplitude increases throughout the whole range of the SL step. Applying the vector model we can explain this behaviour in two stages. The initial rise in the SL absorption leads to a rise in the SL vector's magnitude, which leads to clockwise rotation of the overall SPV vector similar to the QW absorption. After 1.820 eV the SL vector also starts to rotate counterclockwise and this leads to counterclockwise rotation of the overall vector. This behaviour is illustrated in figure 4; inset B, where the overall SPV vector is represented in red for two subsequent SL vectors, following the above scenario. Near the end of the step (1.850 eV), the SL signal is one order of magnitude larger than the signals from the substrate and the QW and it dominates the spectrum. The large magnitude of the SL contribution suggests a gradual transition towards the non-linear recombination regime, which could explain the above-mentioned rotation of the SL vector. This hypothesis is supported by the observed sub-linear SPV dependence on the photon flux density, measured at 1.906 eV shown in figure 6(*a*).

4.2. Samples grown on SI GaAs substrates

Now let us discuss the second set of samples, grown on SI GaAs substrates. Figure 5 shows the typical SPV amplitude and phase spectra. Although the quantum structure is the same for both sets of samples, the SPV amplitude and phase spectra in figure 5 present opposite behaviour as compared with those in figure 4, in the spectral range of the QW and the SL. The QW range reveals dips in the amplitude and peaks in the phase spectrum, while the SL range shows a negative amplitude and a positive phase step. At first glance this result is unexpected, but using the vector model and having in mind the properties of the substrate and the quantum structure we can explain this behaviour as follows.

Because in SI GaAs the energy bands are virtually flat, the dominant cause for SPV generation in the substrate is the Dember voltage effect [2, 26], which relies on the difference in the carrier mobilities. Since the electrons diffuse faster than holes, it gives the SPV phase in the IV quadrant [1, 8]. The amplitude of the substrate signal is much larger as compared with the n-type GaAs substrate, shown in figure 4, and dominates the SPV in the whole spectral range. The peak in the amplitude spectrum at 1.424 eV could be due to absorption from shallow acceptor states to the conduction band [2], but it will not be discussed in this paper. The quantum structure is nominally undoped, but as the most common residual impurity introduced during the MBE growth is carbon, one can expect a slight p-type doping (this effect for the other samples is masked by the high n-type doping of the substrate). Therefore the energy bands at the surface are bent downwards with respect to the bulk. This means that the SPV processes generated from the QW and SL can be manifested by vectors in the II quadrant [8] (see also the discussion in section 3). If these vectors form an obtuse angle with the substrate vector, like the one shown in the vector diagram in figure 5, the growth of their magnitude will result in a decrease in the magnitude and counterclockwise rotation of the overall SPV vector. This is the case for both the QW and the SL spectral ranges, as can be seen from figure 5, where the SPV amplitude decreases and

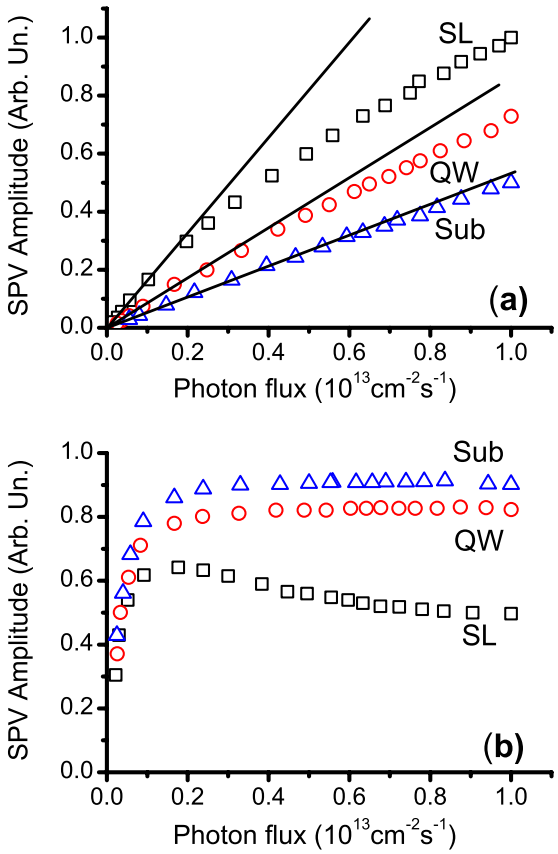

Figure 6. Excitation density dependences of the major spectral features: Substrate (1.530 eV, triangles), QW (1.599 eV, circles) and SL (1.906 eV, squares) for samples grown on (*a*) n-GaAs and (*b*) SI GaAs substrates. The straight lines in (*a*) are a guide for the eye demonstrating the deviation from linearity of the represented dependences. All curves are normalized to different values for clarity.

the SPV phase increases. Due to the large substrate signal, the contribution of the E1-HH1 exciton transitions in the QW is seen as a small dip in the amplitude and a small peak in the phase spectrum, both at 1.603 eV. The E1-LH1 exciton is observed at 1.643 eV in the inset of figure 5, where magnified amplitude and phase spectra are presented. The contribution of the SL is well resolved in figure 5, due to its larger volume—above 1.800 eV one observes a negative step in the amplitude and a positive step in the phase in accordance with the vector diagram in figure 5.

4.3. Intensity dependence

Finally we discuss the excitation density dependences of the major spectral features: substrate (1.530 eV), QW (1.599 eV) and SL (1.906 eV). Figure 6 shows how the SPV amplitude of these features changes with a decrease in the photon flux density from its maximal value $\Phi_{max} = 1 \times 10^{13}$ cm^{-2} s^{-1} used in the spectral runs from figures 4 and 5.

The dependences obtained for the samples with Si doped substrates (figure 6(*a*)) are in accordance with the SPV amplitude and phase spectral behaviour, as discussed above. The dependences obtained for the samples with SI substrates (figure 6(*b*)) are strongly non-linear. The sub-linearity of the curve, corresponding to the substrate photon energy (1.530 eV) is expected, since the Dember voltage effect has a sub-linear dependence on Φ [2]. The contribution of the QW to the SPV signal is relatively small, so the dependence for the QW photon energy (1.599 eV) almost coincides with that of the substrate. At first glance the excitation density dependence for the SL photon energy (1.906 eV) seems to contradict the intuition—reducing the photon flux density leads to an increase in the SPV amplitude. Nevertheless, it can be easily explained by the vector diagram in figure 5, assuming different excitation density dependences for the SL and substrate SPV processes. Indeed the substrate vector itself remains almost unchanged (confirmed by figure 6(*b*)) with decreasing Φ, while the SL vector is expected to decrease. As the angle between these two vectors is obtuse, the net result is an increase in the overall SPV vector magnitude. At very low values of Φ the magnitudes of both vectors obviously decrease towards zero and so does the resulting SPV signal. An increase in the SPV amplitude with decreasing excitation density has been observed in [2], but for sub-bandgap SPV features in bulk SI GaAs samples.

The analysis of the SPV spectral and intensity dependences, presented above, shows that seemingly contradictory SPV results can be well explained, taking into account the behaviour of both SPV amplitude and phase and making use of the proposed vector model.

5. Conclusion

A qualitative vector model is proposed, representing the SPV signal as a radial vector with magnitude equal to the SPV amplitude and angle with respect to the x-axis equal to the SPV phase. It is demonstrated that the model is especially useful when more than one SPV formation process occurs during the spectrum run. The model has been applied to explain the SPV amplitude and phase spectra of two types of samples, containing AlAs/GaAs SL with embedded QWs, grown on different GaAs substrates. The opposite behaviour of the SPV amplitude and phase spectra, observed in the two types of samples has been successfully explained. In this way, important information has been obtained about the investigated SL with embedded QWs and the potential of the proposed model to investigate advanced semiconductor nanostructures has been demonstrated.

The performed analysis emphasizes the need for simultaneous examination of both the SPV amplitude and SPV phase spectra in order to obtain a correct understanding of the experimental data. This study highlights the potential of the SPV spectroscopy in the investigation of complicated nanostructures at room temperature.

Acknowledgments

Financial support from the Bulgarian National Science Fund (contracts U-F-08-04 and VUF-203/06) and the Alexander von Humboldt Foundation, Germany, is acknowledged. The authors thank Denis Martin (EPFL, Switzerland) for supplying the experimental samples.

References

[1] Kronik L and Shapira Y 1999 *Surf. Sci. Rep.* **37** 1
[2] Sharma T K, Kumar S and Rustagi K C 2002 *J. Appl. Phys.* **92** 5959–65
[3] Bhattacharyya J, Ghosh S, Malzer S, Dohler G H and Arora B M 2005 *Appl. Phys. Lett.* **87** 212101
[4] Chan C H, Lee C H, Huang S Y, Wang J S and Lin H H 2007 *J. Appl. Phys.* **101** 103102
[5] Sharma T K, Fox N E, Hosea T J C, Nash G R, Coomber S D, Buckle L, Emeny M T and Ashley T 2008 *Appl. Phys. Express* **1** 062001
[6] Donchev V, Kirilov K, Ivanov Ts and Germanova K 2007 *J. Appl. Phys.* **101** 124305
[7] Ivanov Ts, Donchev V, Wang Y, Djie H S and Ooi B S 2007 *J. Appl. Phys.* **101** 114309
[8] Donchev V, Kirilov K, Ivanov Ts and Germanova K 2006 *Mater. Sci. Eng.* B **129** 186
[9] Schroder D K 2001 *Meas. Sci. Technol.* **12** R16–R31
[10] Sharma T K, Porwal S, Kumar R and Kumar S 2002 *Rev. Sci. Instrum.* **73** 1835
[11] Touskova J, Samochin E, Tousek J, Oswald J, Hulicius E, Pangrac J, Melichar K and Simecek T 2002 *J. Appl. Phys.* **91** 10103
[12] Liang J S, Wang S D, Huang Y S, Tien C W, Chang Y M, Chen C W, Li N Y, Tiong K K and Polak F H 2003 *J. Phys: Condens. Matter* **15** 55–66
[13] Datta S, Arora B M and Kumar S 2000 *Phys. Rev.* B **62** 13604
[14] Dumitras G, Riechert H, Porteanu H and Koch F 2002 *Phys. Rev.* B **66** 205324
[15] Zhang Y, Xie T, Jiang T, Wei X, Pang S, Wang X and Wang D 2009 *Nanotechnology* **20** 155707
[16] Olafsson H O, Gudmundsson J T, Svavarsson H G and Gislason H P 1999 *Physica* B **273–4** 689–92
[17] Kumar, Ganguli T, Bhattacharya P and Roy U N 1998 *Appl. Phys. Lett.* **72** 3020–2
[18] Donchev V, Shtinkov N, Germanova K, Ivanov I, Brachkov H and Ivanov T 2001 *Mater. Sci. Eng.* C **15** 75
[19] Shtinkov N, Donchev V, Germanova K, Vlaev S and Ivanov I 2000 *Vacuum* **58** 561
[20] Donchev V, Germanova K, Shtinkov N and Vlaev S J 2006 *Electronic structure and optical properties of AlAs/GaAs superlattices containing embedded GaAs quantum wells with abrupt and graded interfaces* ed O T Chang (New York: Nova Science) pp 25–60
[21] Blood P 1991 *Physics and Technology of Heterojunction Devices* ed D V Morgan and R H Williams (London, UK: Peter Perigrinus) p 231
[22] Ryvkin S M 1964 *Photoelectric Effects in Semiconductors* (New York: Consultants Bureau) p 31
[23] Ivanov Ts, Donchev V, Kirilov K and Germanova K 2007 *J. Optoelectron. Adv. Mater.* **9** 190–3
[24] Ruda H and Shik A 2002 *J. Appl. Phys.* **91** 6476
[25] Liu Q, Ruda H E, Chen G M and Simard-Normandin M 1996 *J. Appl. Phys.* **79** 7790
[26] Liu Q, Chen C and Ruda H 1993 *J. Appl. Phys.* **74** 7492